

THEORETICAL PERFORMANCE OF THE NON-COHERENT AIR-RECEIVER

Alois M.J. Goiser

TU-Vienna

Institut für Allgemeine Elektrotechnik und Elektronik
Abteilung für Angewandte Elektronik
E-mail: agoiser@ps1.iaee.tuwien.ac.at.

ABSTRACT

The theoretical performance of the non-coherent AIR-receiver depicted in [1], [2] is investigated and compared to other digital receivers of low complexity, the RIR- and HL-receiver [1], [2]. As interference is assumed that the weak direct-sequence signal is corrupted with additive white gaussian noise and a coherent, constant envelope continuous wave. The theoretical performance is derived with the assumption that the adaptive 2-bit nonlinearity has adjusted its magnitude threshold at the optimum location. The bit-error-rate for constant signal-to-interference ratio and variable signal-to-noise ratio is presented.

INTRODUCTION

The present paper focus on the theoretical bit-error rate for the non-coherent AIR-receiver. The AIR-receiver is a member of the class of digital receivers of low-complexity and integrated interference reduction and uses orthogonal signaling. An overview of this class of receivers is sketched in Fig.1. The theoretical performance of the AIR-receiver is compared to the RIR-receiver, which uses a different adaptive interference reduction scheme and the simple HL-receiver, which is the member with lowest complexity and no interference reduction capability.

The interference environment is a composition of a permanently present wideband process, modelled as additive white gaussian noise (AWGN), and a permanently present narrowband process, modelled as continuous-wave (CW) interference. We will refer to this type of interference as *combined interference*. The analysis is done for a wide range of interference compositions. It spans the interference environment from dominating AWGN-interference to dominating CW-interference.

In the next section a brief review of the AIR-receiver is given from [1]. The RIR- and HL-receiver are depicted in [2]. After the brief introduction to the receivers the performance of the non-coherent AIR-receiver is presented and discussed.

AIR-RECEIVER

The interference reduction capability of the AIR-receiver is based on estimating the interference composition by exploiting level-crossing- and amplitude statistics. This allows for adapting the amplitude-thresholds close to the op-

imum threshold location and track it, if the composition of the interference changes. In this way it is an adaptive interference reduction (AIR) scheme. We refer to a receiver using this scheme as *AIR-receiver* (Adaptive Interference Reduction). The weighting-factor is dependent on the threshold location and derived from the control variable. Owing to this, we reduce the amount of weighted faulty chip-decisions, which cause an increase in performance. A block-diagram of the AIR-receiver is sketched in Fig.2.

$$\begin{aligned} s(t) &= A_{cw} \sin(2\pi f_{cw}t + \varphi) + n(t) + A_c d(t) c(t) = \\ &= i(t) + n(t) + s_T(t) \end{aligned} \quad (1)$$

The received and downconverted signal $s(t)$ in (1) consists of a weak direct-sequence signal $c(t)$ corrupted by a strong CW-signal $A_{cw} \sin(\omega t + \varphi)$ with arbitrary phase φ , yielding the input $SINR_s$ to the nonlinearity.

$$SINR_s = \frac{\mathbf{E} [c^2(t)]}{\mathbf{Var} [i(t)] + \mathbf{Var} [n(t)]} = \frac{2 \cdot A_c^2}{A_{cw}^2 + 2 \cdot \sigma_N^2}. \quad (2)$$

The behavior of the ADC^(2A)-nonlinearity, its transfer characteristic and the signal mapping is depicted in [1] and the optimum threshold location is found to be:

$$\Delta_{opt} = A_{cw} - A_c \quad (3)$$

The weighting scheme is presented in [1], [2].

PERFORMANCE

The performance of the proposed AIR-receiver is quantified with the bit-error rate. The bit-error rate of the investigated receiver is compared to the simple HL-receiver and the RIR-receiver.

The assumptions for the derivative of the bit-error rate are, that the amplitude thresholds are at their optimum locations (3) and the spread-spectrum synchronization is established. The dynamic (variation in $SINR$) is not included. This means that for a new interference situation the corresponding optimum amplitude locations are achieved with infinite speed.

The bit-error rates depicted in Fig.3 are theoretical bit-error rates. The calculation of the $SINR_z$ at the detector

input for the non-coherent receiver is approximated by the following derivation. The calculation is done on a chip bases. The variables used in the derivation correspond with the variables in Fig.2. We have to distinguish between the I - and Q -channel. The signal in the I -channel for a positiv chip after ideal downconversion for a certain fixed CW-phase φ is:

$$A_c^{(I)} = A_c \cdot \cos\left(\frac{2\pi}{360} \cdot \varphi\right) \quad (4)$$

With this signal component we feed the adaptive 2-bit ADC. The expectation $\mathbf{E}[V_I]$ and the variance $\mathbf{Var}[V_I]$ of the random-variable V_I are prepared with $P_{R,I}, P_{1,I}, P_{-1,I}, P_{-R,I}$ and given in (5) and (7).

$P_{R,I}$ Probability that the signal in the I-channel is weighted with R .

$P_{1,I}$ Probability that the signal in the I-channel is greater than zero and less then the magnitude threshold Δ .

$P_{-1,I}$ Probability that the signal in the I-channel is less than zero and greater then the magnitude threshold $-\Delta$.

$P_{-R,I}$ Probability that the signal in the I-channel is weighted with $-R$.

After the digital matched-filter we have (8) and (9) and squaring yields (10) to (12).

$$\mathbf{E}[V_I] = P_{1,I} - P_{-1,I} + R' \cdot [P_{R,I} - P_{-R,I}] \quad (5)$$

$$\mathbf{E}[V^2] = P_{1,I} + P_{-1,I} + R'^2 \cdot [P_{R,I} + P_{-R,I}] \quad (6)$$

$$\mathbf{Var}[V_I] = \mathbf{E}[V_I^2] - \mathbf{E}^2[V_I] \quad (7)$$

$$\mathbf{E}[B_{I,1}] = G_p \cdot \mathbf{E}[V_I] \quad (8)$$

$$\mathbf{Var}[B_{I,1}] = G_p \cdot \mathbf{Var}[V_I] \quad (9)$$

$$\mathbf{E}[F_{I,1}] = \mathbf{Var}[B_{I,1}] + \mathbf{E}^2[B_{I,1}] \quad (10)$$

$$\mathbf{E}[B_{I,1}^4] = \mathbf{E}^4[B_{I,1}] + 6\mathbf{E}^2[B_{I,1}] \cdot \mathbf{Var}[B_{I,1}] + 3\mathbf{Var}[B_{I,1}] \quad (11)$$

$$\mathbf{Var}[F_{I,1}] = \mathbf{E}^4[B_{I,1}] - \mathbf{E}^2[B_{I,1}] \quad (12)$$

The same processing for a positive chip happens in the Q -channel leading to $\mathbf{E}[F_{Q,1}]$ and $\mathbf{Var}[F_{Q,1}]$. The expectation and variance of the random variable U_1 after I/Q -combining is shown in (13) and (14) respectively.

$$\mathbf{E}[U_1] = \mathbf{E}[F_{I,1}] + \mathbf{E}[F_{Q,1}] \quad (13)$$

$$\mathbf{Var}[U_1] = \mathbf{Var}[F_{I,1}] + \mathbf{Var}[F_{Q,1}] \quad (14)$$

The decision statistic for the quadratic detector is represented by the $SINR_z^{(QD)}$ in (15) with $\mathbf{E}[Z] = \mathbf{E}[U_1] - \mathbf{E}[U_0]$.

$$SINR_z^{(QD)} = \frac{\mathbf{E}^2[Z]}{\frac{1}{2} \cdot (\mathbf{Var}[U_1] + \mathbf{Var}[U_0])} \quad (15)$$

In order to calculate the bit-error rate for a certain phase, we approximat the signal-to-noise ratio from the quadratic detector in (15) for the equivalent signal-to-noise ratio feed to a linear detector (16). The bit-error rate for a fixed phase is given in (17) and averaged over all possible phases to form the average bit-error rate in (18).

$$SINR_z^{(LD)} = SINR_z^{(QD)} + \sqrt{\left(SINR_z^{(QD)}\right)^2 + SINR_z^{(QD)}} \quad (16)$$

$$P_e^{(\varphi)} = \frac{1}{2} \cdot e^{-\frac{1}{2} \cdot SINR_z^{(LD)}} \quad (17)$$

$$P_e = \mathbf{E}[P_e^{(\varphi)}] = \frac{1}{2\pi} \int_{\varphi=0}^{2\pi} P_e^{(\varphi)} d\varphi \quad (18)$$

All investigated and compared receivers are using the same processing gain and are tested in the same combined interference.

In order to make a fair comparison, the assumed parameters for the RIR-receiver are set to $psm = 20\%$, $R' = 4$ and the parameter setting for the AIR-receiver is: $k_r = 1$, $R = 4$, yielding the same $R' = 4$.

In Fig.3 the bit-error rates of the investigated receivers are sketched and compared to the corresponding analog counterpart. Curve 1 shows the bit-error rate of an analog receiver in pure AWGN-interference. This curve is the maximum achievable CW-interference reduction that is possible and the term CW-supression is suitable.

The AIR-receiver shows its superiority in reducing the CW-interference and outperforms all his digital counterparts.

CONCLUSION

It was shown that the theoretical bit-error rate for the AIR-receiver is always better as the bit-error rate of the RIR-receiver and the simple HL-receiver. This was achieved with the adaptive interference reduction strategie with the optimally adjusted magnitude thresholds-pair. Estimating the composition of the interference with the aid of the level-crossings is a powerful scheme to reduce CW-interference.

ACKNOWLEDGEMENT

The author is thankful to Prof. Franz Seifert for his continuous encouragement during this project and his useful comments.

REFERENCES

- [1] A. Goiser, *Interference Reduction Using Manipulated Signal Statistics*, Proc. IEEE-ISSTA'96, (1996).
- [2] A. Goiser, *Enhanced Continuous Wave Interference Reduction in Low Complexity Digital Direct-Sequence Spread-Spectrum Receivers*, Proc. IEEE-Milcom'96, (1996).

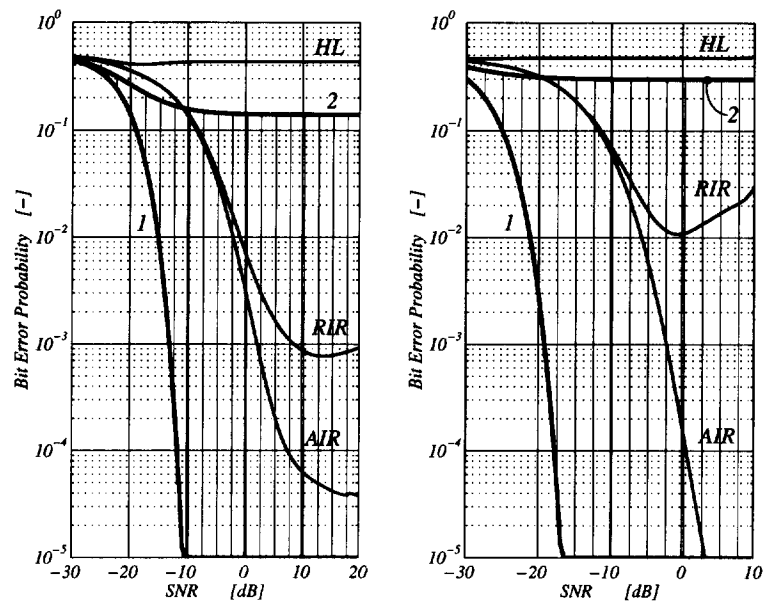


Figure 3. A Comparison of bit error rates in combined interference for the AIR-, RIR-, HL-receiver and analog receiver. *Left*: All the presented receivers have a processing gain of 255 chips. The *SIR* is constant -20 dB. The parameters for the AIR-receiver are: $R = 4, k_r = 1$. The RIR-receiver uses the following settings: $pshm = 20$ and $R = 4$. An analog receiver in pure AWGN-interference is shown in curve 1 and in equivalent combined interference in curve 2. *Right*: All the presented receivers have a processing gain of 1023 chips. The *SIR* is constant -30 dB. The parameters for the AIR-receiver are: $R = 4, k_r = 1$. The RIR-receiver uses the following settings: $pshm = 20$ and $R = 4$. An analog receiver in pure AWGN-interference is shown in curve 1 and in equivalent combined interference in curve 2. .